

# Synthesis and materials properties of transparent conducting $\text{In}_2\text{O}_3$ films prepared by sol–gel-spin coating technique

E. Savarimuthu<sup>a</sup>, K.C. Lalithambika<sup>d</sup>, A. Moses Ezhil Raj<sup>c</sup>, L.C. Nehru<sup>b</sup>,  
S. Ramamurthy<sup>c</sup>, A. Thayumanavan<sup>e</sup>, C. Sanjeeviraja<sup>b</sup>, M. Jayachandran<sup>f,\*</sup>

<sup>a</sup>Department of Physics, Gandhigram Rural Institute-Deemed University, Gandhigram 624 302, India

<sup>b</sup>Department of Physics, Alagappa University, Karaikudi 630 003, India

<sup>c</sup>Department of Physics, Scott Christian College, Nagercoil 629 003, India

<sup>d</sup>Department of Physics, SASTRA University, Thirumalai Samudram 613 402, India

<sup>e</sup>AVVM Sri Pushpam College, Poondy 613 503, India

<sup>f</sup>ECMS Division, Central Electrochemical Research Institute, Karaikudi 630 006, India

Received 12 January 2007; received in revised form 21 February 2007; accepted 21 February 2007

## Abstract

Transparent conducting indium oxide ( $\text{In}_2\text{O}_3$ ) thin films have been prepared on glass substrates by the simple sol–gel-spin coating technique. These films have been characterized by X-ray diffraction, resistivity and Hall effect measurements, optical transmission, scanning electron microscopy and atomic force microscopy for their structural, electrical, optical and morphological properties. The influence of spin parameters, number of coating, process temperature on the quality of  $\text{In}_2\text{O}_3$  films are studied. In the operating range of deposition, 400–475 °C, all the films showed predominant (2 2 2) orientation. Films deposited at optimum process conditions exhibited a resistivity of  $2 \times 10^{-2} \Omega \text{cm}$  along with the average transmittance of about 80% in the visible spectral range (400–700 nm).

© 2007 Elsevier Ltd. All rights reserved.

**Keywords:** A. Thin films; C. X-ray diffraction

## 1. Introduction

Indium oxide (IO) is a wide band gap (direct band gap energy of 3.4–3.75 eV) transparent conducting semiconductor and has C-type rare earth sesquioxide structure with space group  $T_h^7$  ( $\text{Ia}\bar{3}$ ) containing 80 atoms or 16 formula units. This structure is related to a fluorite in which one-fourth of all anion sites are structurally vacant [1]. Due to its wide band gap, it transmits visible radiation efficiently. Stoichiometric  $\text{In}_2\text{O}_3$  is an insulator, which becomes highly conducting in its non-stoichiometric  $\text{In}_2\text{O}_{3-x}$  form due to oxygen deficiency. Each oxygen vacancy will behave like a doubly or singly ionized donor, which makes IO to exhibit high electrical conductivity similar to heavily doped degenerate n-type semiconductor and one of the technolo-

gically more important materials because of its utility in diverse applications. It shows excellent electrical and optical properties suitable for the use as transparent electrodes in devices such as multi-layer solar cells, flat panel displays and photodiodes [2,3]. In thin film form, their wide ranges of applications include transparent windows in liquid crystal displays, anti-reflection coatings [4], optoelectronic and electrochromic devices [5] and has shown remarkable prospects in the field of upcoming nanoelectronic building blocks and nanosensors. The observance of both high optical transmittance and high electrical conductivity simultaneously in IO makes it a suitable transparent conducting oxide material for many devices developments [6,7]. In device applications, due to its wide band gap nature,  $\text{In}_2\text{O}_3$  form heterostructures with many semiconductors [8–11] like Si, GaAs and InP. Recently, non-stoichiometric IO films have been used for gas sensors and related devices [12–14]. The interest in

\*Corresponding author. Tel.: +91 4565 227550 59x218.

E-mail address: [jayam54@yahoo.com](mailto:jayam54@yahoo.com) (M. Jayachandran).

$\text{In}_2\text{O}_{3-x}$  mainly emanates from the prospects of reducing the electrical resistivity by about 10 orders of magnitude by varying the oxygen vacancy alone [15].

$\text{In}_2\text{O}_3$  thin films can be prepared by a variety of techniques such as chemical vapor deposition (CVD) [16,17], reactive thermal evaporation [18,19], pulse laser deposition (PLD) [20,21], ion beam sputtering [22], RF/direct current (DC) magnetron sputtering [23,24], spray pyrolysis [25,26], thermal decomposition of precursors [27], thermal and UV-assisted sol–gel dip coating technique [28]. The structural, optical and electrical properties are highly sensitive to the preparation technique, preparation temperature and post heat treatment temperature. The evaporation, sputtering and laser ablation techniques are expensive for large area films production and for industrial applications. The sol–gel route is simple and capable of providing an easy route to fabricate thin films of good quality over large areas and better-controlled composition [29,30] without the need for any sophisticated equipment. Further, the sol–gel-spin (SGS) coating technique offers a competitive alternative for the mass production of transparent conducting oxide films like  $\text{In}_2\text{O}_3$  with low cost.

As far as to the authors' knowledge, this is the first ever report on the production of  $\text{In}_2\text{O}_3$  films by the SGS coating technique. The aim of this work is to optimize the SGS coating process to prepare device quality  $\text{In}_2\text{O}_3$  films. In a first step, we optimized the SGS procedure, then other important oxide film formation parameters such as concentration of precursors and heat treatment temperature were uniquely fixed. This paper presents the results on the structural, optical, electrical and morphological properties of  $\text{In}_2\text{O}_3$  films formed on glass substrates.

## 2. Experimental methods

The indium oxide (IO,  $\text{In}_2\text{O}_3$ ) thin films of the present study have been prepared through the SGS coating technique using an indigenously developed microcontroller-based spin coater. The precursor solution for preparing the sol–gel has been prepared by dissolving the desired amount (Section 3.1) of the precursor salt indium III chloride in 100 ml of ethanol adding 5 ml of hydrochloric acid (HCl). The solution is refluxed at 60 °C for 1 h. Now the sol is ready. It is kept in an open beaker for gelation. After 3 days of gelation, the sol–gel is used for coating. Successive coatings have been made on the same glass substrate to obtain considerable film thickness. After each coating it is air-dried first and then subjected to heat treatment separately to avoid cracking [31]. The preparation of these films has been carried out by optimizing the process parameters such as the solute concentration, gelation time, turn table spin rate and time, number of coatings (i.e. film thickness) and process temperature (i.e. the heat treatment temperature). The structural characterization of the films has been done using the X'pert pro, Netherland X-ray diffractometer (XRD). The surface morphological studies have been made using JSM 35 CF

JEOL scanning electron microscope (SEM) and Nano-scope<sup>®</sup> E Scanning Probe Microscope system Model No.3138 J [atomic force microscope (AFM)]. Using a Perkin-Elmer Lambda35 UV–Vis–NIR Spectrophotometer optical spectra are recorded. The electrical resistivities of the films were measured using Four Probe resistivity apparatus and the Hall effect measurements have been made using a Hall effect set-up.

## 3. Results and discussion

### 3.1. Optimization of SGS coating process

#### 3.1.1. Optimization of solute concentration

The precursor salt (solute) concentration has a strong influence on the film formation, its transparency and quality and hence the solute concentration has been optimized for obtaining well adherent films. Initially, when 0.035 mol% of indium chloride ( $\text{InCl}_3$ ) was used in the sol–gel preparation, the indium oxide film formed had powdery layer on top, which could be gently wiped off. Totally 9 coatings have been given and for every coating the above process has been adopted. A foggy lusterless film with a high resistivity of 0.30  $\Omega\text{cm}$  and a high thickness of 280 nm has been obtained. When the precursor salt concentration was reduced to 0.03, 0.025 mol%, the thickness of the powdery layer became less and the resistivity got progressively lowered; however, the film thickness was more or less constant. At 0.02 mol% solute concentration, there is no powdery layer formation at all and a fairly transparent  $\text{In}_2\text{O}_3$  film with good luster, with slightly reduced thickness but a lower resistivity of 0.05  $\Omega\text{cm}$  could be obtained. When the precursor salt concentration was 0.015 mol% a good uniform indium oxide film with very good luster, very low resistivity of 0.04  $\Omega\text{cm}$  and a transmittance of 74% has been obtained. Now the film thickness is marginally reduced. When the solute concentration was still further reduced to 0.01 mol%, uniform films with very good luster and high transparency existed in the  $\text{In}_2\text{O}_3$  films but the film thickness falls sharply and the resistivity raised. The variation of thickness ( $h$ ) and resistivity ( $\rho$ ) of the  $\text{In}_2\text{O}_3$  films with solute concentration can be explained as follows.

When the indium chloride solute concentration is fairly high (0.035 mol%) the excess solute atoms may come out of the film and form the top powdery layer, the film may still have more solute atoms and as a result there could be very limited oxide formation resulting in a foggy film with high resistivity and high thickness. When the solute concentration decreases, these effects will be reduced resulting in more oxide formation and more oxygen vacancies and hence film resistivity decreases. At a particular precursor salt concentration (0.015 mol% in this case) all the atoms in the film will be oxidized and well crystallized so that the resistivity will be minimum, the film luster will be good and transmittance will be high which is the optimum solute concentration. When the solute concentration is reduced

further to 0.01 mol% though oxide formation is there and though the transparency and luster may be good, due to lower number of solute atoms, the number of oxygen vacancies may be lowered due to complete oxidation and hence the resistivity may rise and thickness fall.

### 3.1.2. Fixation of the gelation time/aging time

Gelation time/aging time of the sol is an important parameter that has been optimized to obtain well adherent coatings using the sol–gel process. Savarimuthu et al. [32] have established that the density variation with the gelation/aging time could be used for fixing the gelation stage for good coating. The variation of density of the sol with gelation time/aging is shown in Fig. 1.

The density of the sol rises slowly for the first 3 days of aging and then rises more rapidly indicating the onset of the gelation process (called the break-off time) and the density rises more or less uniformly up to 7 days of aging. Between 7 and 12 days of aging, the rise is not uniform and after 12 days, it tends to a saturation stage (called the saturation time) indicating that the gelation stage is complete and thick gel is formed. After 7 days of aging (density of the sol–gel  $1.245 \text{ g cm}^{-3}$ ), the coating becomes non-uniform which progressively became highly irregular and after 12 days, the material was completely thrown off the substrate without any coating sticking to the glass substrate. When the sol of less than 2 days of aging is used, ultra thin films alone could be obtained. However, good coating could be obtained between 3 and 7 days of gelation. From their TEM study, Lin and Wu [30] have shown that the particle size increases with aging. It seems that very heavy particles corresponding to near complete gelation stage are unable to adhere to the substrate due to very high density and viscosity and perhaps only the sol–gel aged between 3 and 7 days (density  $0.942\text{--}1.245 \text{ g cm}^{-3}$ ) has optimum particle size to produce uniform and device quality films. Based on this fact, a gelation time of 3 days has been fixed for preparing  $\text{In}_2\text{O}_3$  films in the present work.

### 3.1.3. Selection of the spin rate ( $\omega$ )

The spin rate ( $\omega$ ) affects the degree of the centrifugal force applied to the sol–gel and the velocity and

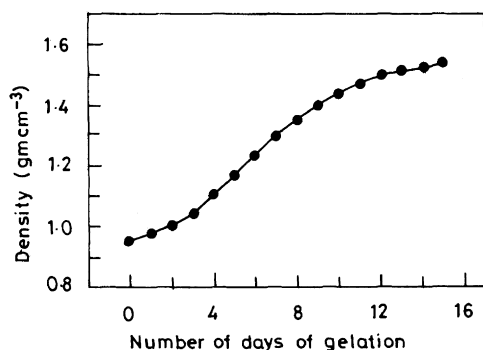


Fig. 1. Variation of density of the gel with number of days of gelation.

characteristics turbulence of the air immediately above it, and hence the spin rate has a strong influence on the film thickness. So the spin rate of the turn table was optimized for getting quality films with optimum thickness.

The variation of resistivity ( $\rho$ ) and film thickness ( $h$ ) of the  $\text{In}_2\text{O}_3$  films with spin rate ( $\omega$ ) measured in the interval of 500 rpm from 2000 to 4000 rpm are shown in the Fig. 2. At a fairly low spin rate of 2000 rpm, the indium oxide film formed had several islands with pale yellowish contours, poor uniformity and poor luster. This may be due to the irregular outward flow of the sol–gel due to the lower degree of the centrifugal force acting on the sol–gel which results in non-uniform thinning of the sol–gel on the substrate. At this stage, the resistivity and film thickness are high. When the spin rate increases, the island formation is lowered and the film uniformity and luster improved much however the thickness falls. This could be attributed to the better uniform outward flow of the sol–gel due to enhanced degree of centrifugal force on the sol–gel. Less island formation (i.e. better film uniformity) may tend to decrease the sheet resistance while the thickness reduction will tend to increase the sheet resistance. When the spin rate is increased from 2000 rpm, perhaps the contribution from the first effect may contribute more than the second and hence the film resistivity falls progressively. At 3500 rpm, good uniform films without any island formation have been obtained and the resistivity reaches a minimum. At spin rates above 3500 rpm, most of the sol–gel is thrown out due to high degree of centrifugal force resulting in very thin films at which stage the contribution to sheet resistance due to the second effect becomes

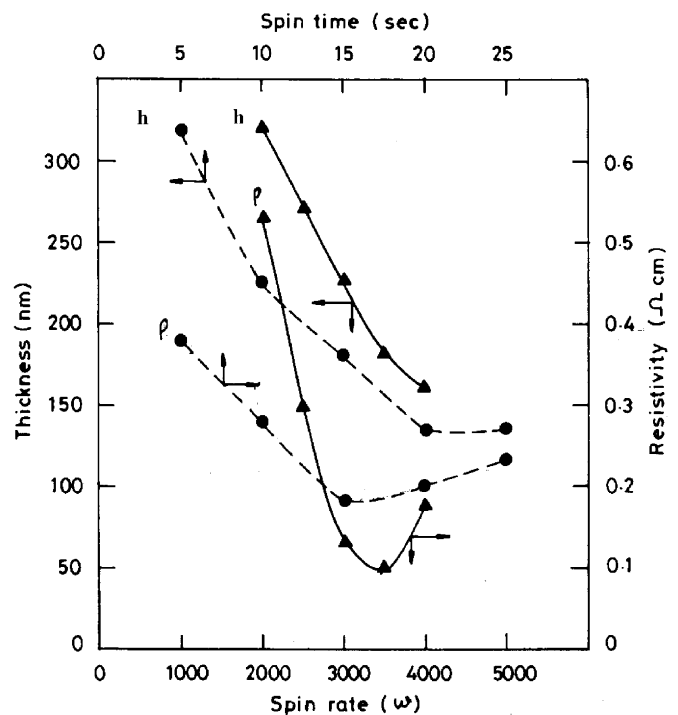


Fig. 2. Variation of thickness ( $h$ ) and resistivity ( $\rho$ ) with (a) spin rate ( $\blacktriangle$ ) and (b) spin time ( $\bullet$ ) of IO films (9 coatings).

dominant and hence the sheet resistance and consequently the resistivity increases. So a spin rate of 3500 rpm is selected for preparing  $\text{In}_2\text{O}_3$  films of the present study.

### 3.1.4. Standardization of spin time

Keeping the number of coatings, process temperature and turn table spin rate at 8 coatings,  $425^\circ\text{C}$  and 3500 rpm, respectively, and varying the turn table spin time ( $t$ );  $\text{In}_2\text{O}_3$  films of different thickness have been prepared. The resistivity ( $\rho$ ) and thickness ( $h$ ) of these films as a function of the spin time ( $t$ ) are shown in Fig. 2. When a spin time of 5 s was used, the films had uneven surface, poor luster and a large number of islands with pale yellowish boundary grains, the resistivity was relatively high and film thickness was also relatively high. With increasing spin time, the surface smoothness, uniformity and luster improved and the area of islands got reduced, both resistivity and film thickness registered a fall. When the spin time was fixed at 15 s, uniform films without any island formation could be obtained whose resistivity value reached a minimum of about  $0.17\ \Omega\text{cm}$ . Above this spin time, the resistivity increased while a marginal decrease in thickness was observed. Hence, a spin time of 15 s is found suitable for preparing quality  $\text{In}_2\text{O}_3$  films.

### 3.1.5. Comparison between theoretical prediction and experimental results on the variation of film thickness ( $h$ ) with the spin rate ( $\omega$ ) and spin time ( $t$ )

Daughton and Givens [33] and Hirasawa et al. [34] have separately proposed a simple theoretical model for the spin coating process, according to which, the film thickness ( $h$ ) is given by the relation

$$h = \frac{h_0}{[1 + (4\pi\rho\omega^2 h_0^2 t)/\eta]^{1/2}} \quad (1)$$

where  $h_0$  is the value of  $h$  at time  $t = 0$ .

For larger  $t$ ,  $(4\pi\rho\omega^2 h_0^2 t)/\eta \gg 1$

$$h = [\eta/4\pi\rho\omega^2 t]^{1/2}. \quad (2)$$

This equation shows that film thickness ( $h$ ) is inversely proportional to  $\omega$  and also inversely proportional to the square root of ( $t$ ).

Following Peurrung and Graves [35], if it is assumed that drying/heat treatment has no significant effect on the shape of the film profile, then the thickness of the dried and heat-treated  $\text{In}_2\text{O}_3$  films may be taken to be reasonably valid and proportional to  $(1/\sqrt{t})$  and  $(1/\omega)$ .

Fig. 3 shows the experimental values of the variation in thickness with  $1/\omega$  and  $1/\sqrt{t}$  for the  $\text{In}_2\text{O}_3$  films which are more or less straight lines showing a linear variation. These experimental results of our SGS coated films are found in good agreement with the simple theoretical predictions of spin coating process.

The variation of the  $\text{In}_2\text{O}_3$  film thickness with number of coatings was studied and a linear relationship between film thickness and number of coatings is observed. Thickness of the films for 6, 7, 8, 9 and 10 coatings were observed as 202,

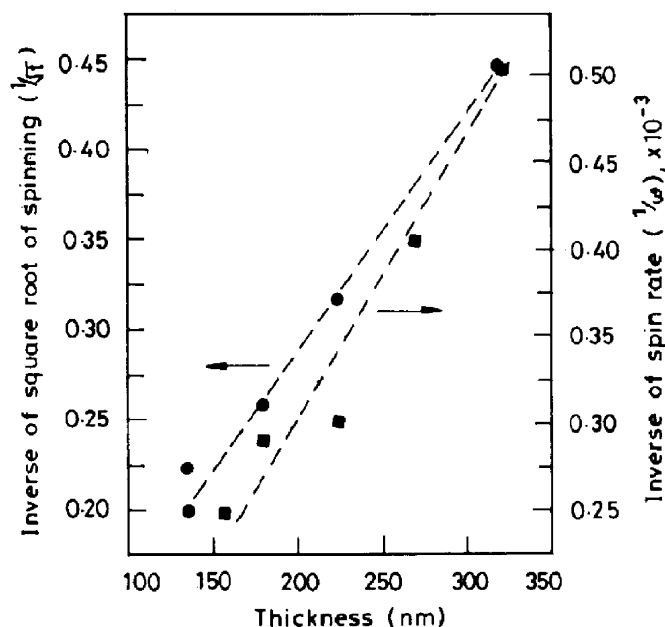


Fig. 3. Variation of thickness with  $1/\omega$  and  $1/\sqrt{t}$ .

225, 247, 269 and 292 nm, respectively. Such a trend has been reported by Lee et al. [36] and Savarimuthu et al. [32] for SGS coated  $\text{SnO}_2$  films and Sankarasubramanian et al. [37] for their FTO films. There is practically no distinguishable change in film thickness when the heat treatment temperature is varied in the range of  $400\text{--}475^\circ\text{C}$ . Such a result has been reported by other investigators for  $\text{SnO}_2$ -based films [36,37]. The average growth rate of the spin coated  $\text{In}_2\text{O}_3$  films is about  $30\ \text{nm/coat}$ .

### 3.2. Effect of (film thickness) number of coatings on film characteristics

The nature and quality of an oxide semiconductor film mainly depends on its thickness due to the fact that it modifies the atomic orientations, defect structures and the resulting electrical properties. The variations of structural, electrical and optical properties with number of coatings are studied.

#### 3.2.1. Structural studies

The XRD patterns of the SGS coated  $\text{In}_2\text{O}_3$  thin films of the present study developed by varying the number of coatings are shown in Fig. 4a. It shows that all the films are polycrystalline with the most preferred orientation along (2 2 2), other peaks corresponding to (2 1 1), (4 0 0), (4 1 1), (4 4 0) and (6 2 2) orientations are also available. These peaks are characteristic of  $\text{In}_2\text{O}_3$  crystallites with bcc structure. The lattice parameters for all the films work out to be  $10.11(2)\ \text{\AA}$  which is in very good agreement with the value of  $10.11\ \text{\AA}$  obtained by Parent et al. [38] for  $\text{In}_2\text{O}_3$  crystals. Following Mergel et al. [39] and Ghosh et al. [40], it can be concluded that since the spin coating method does not involve any particle bombardment of the growing

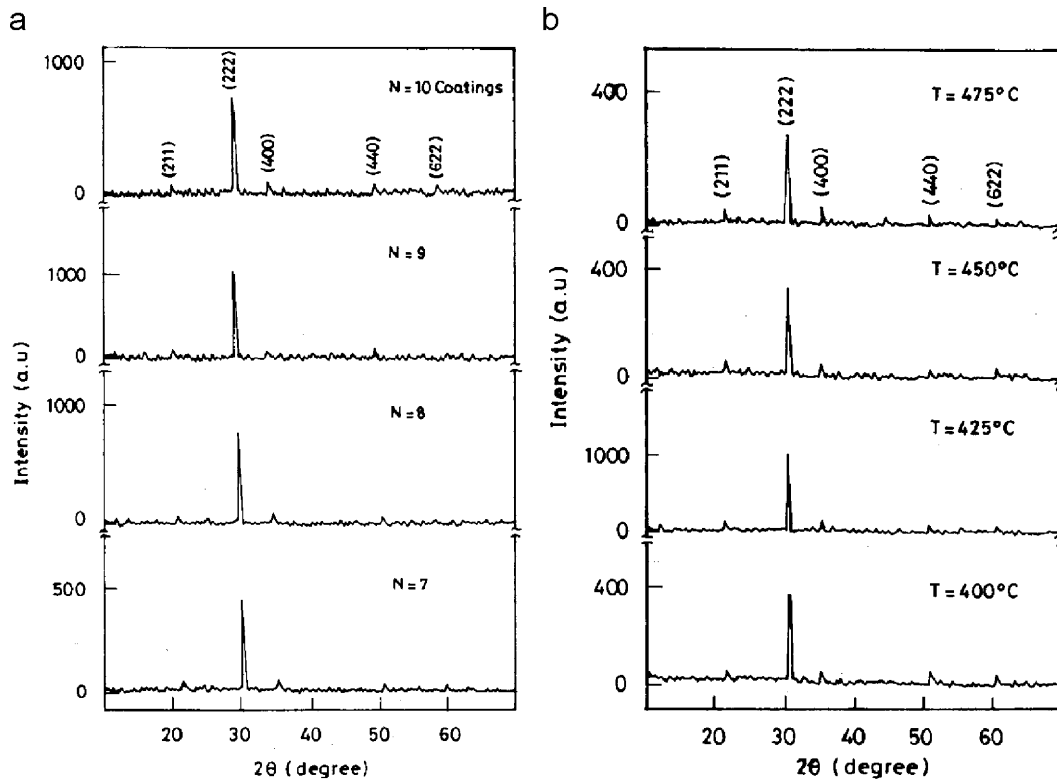


Fig. 4. XRD spectra of (a) IO films with different number of coatings ( $N$ ) and (b) different heat treatment temperatures ( $T$ ) for IO films (9 coatings).

films, the major peak reflection is along (222) orientation. From these XRD patterns, it can be seen that as the number of coatings increases up to 9 coatings the (222), (221) and (400) peak intensities increase and beyond this stage the intensity falls. When the number of coatings increases, the number of heat treatment steps and hence the total time duration of heat treatment for film consolidation also increases. So there could be marked improvement in crystallinity and/or in the crystallite size, and the XRD peak intensity would increase with the number of coatings. However, on this count, the fall of XRD intensity after the 9th coating is rather surprising. This decrease of the XRD intensity beyond 9 coatings may be taken to indicate lattice or realignment of crystallites in the lattice [32].

### 3.2.2. Electrical studies

Hall measurements indicate that all the  $\text{In}_2\text{O}_3$  films heated at  $425^\circ\text{C}$  are n-type semiconductors. The variation of the carrier concentration ( $n$ ) and mobility ( $\mu$ ) with the number of coatings along with the variation of resistivity ( $\rho$ ) of the films is represented in Fig. 5. It can be observed that as the number of coatings increases the carrier concentration ( $n$ ) and a mobility ( $\mu$ ) value show an increase and reach a maximum value of  $2.22 \times 10^{19} \text{cm}^{-3}$  and  $14.0 \text{cm}^2/\text{Vs}$ , respectively, at 9 coatings and then fall, the resistivity falls and reaches a minimum value of  $0.02 \Omega \text{cm}$  at 9 coatings and then rises. When the number of coatings increases, the increase of film thickness and the improvement in the crystallinity and/or the size of the crystallite

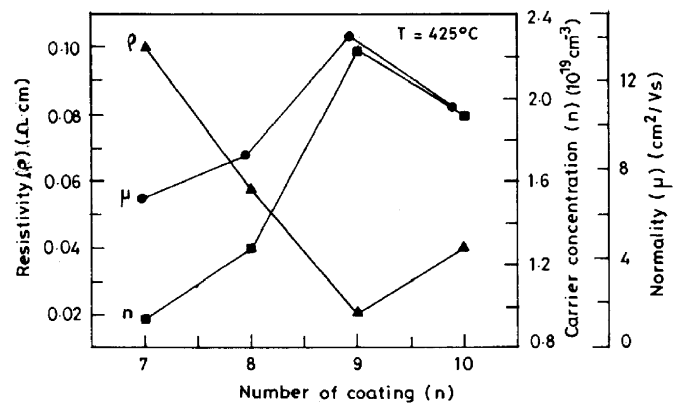


Fig. 5. Variation of carrier concentration ( $n$ ), mobility ( $\mu$ ) and resistivity ( $\rho$ ) of IO films with number of coatings.

result in the availability of greater number of atoms and reduction of scattering centers which would, as an aiding factor, tend to improve the electrical characteristics of the film. It can be stated that because of the dominance of the aiding factor, there is increase in the carrier concentration, mobility and conductivity as the number of coatings increases. However, the increase in the number of heat treatment steps would lead to a reduction in the number of oxygen vacancies, which in turn would tend to deteriorate the carrier concentration and conductivity. It can be stated that because of the predominance of the above-mentioned aiding factor, there is increase in the carrier concentration,

mobility and conductivity as the number of coatings increases. But the XRD studies show that there is some lattice disorder and atomic rearrangements in the crystallites after 9 coatings. This factor may also tend to deteriorate the electrical characteristics of the films. These deteriorating factors may become dominant over the aiding factor after the 9th coating and hence the carrier concentration, mobility and conductivity would fall after this stage.

### 3.2.3. Optical studies

The transmittance spectra of the  $\text{In}_2\text{O}_3$  thin films recorded in the wavelength range of 300–700 nm for different number of coatings are shown in Fig. 6. The figure indicates that all the films with the number of coatings between 7 and 10 (film thickness between 225 and 292 nm) have more or less the same optical transmittance in the visible region. The porosity, crystallinity, structural and surface homogeneity greatly influence the film transmission [41]. When the number of coatings is small say 1 or 2 coatings (the film thickness is approximately 22–44 nm in this case) the porosity will be high which will tend to increase the transmittance; at the same time, the crystallinity and surface and structural homogeneity may be poor tending to reduce the transmittance; but because of the dominance of the effect due to porosity, the transmittance could be high. This is in agreement with the contention of Kim et al. [41] that low film thickness results in enhanced transmission. However, when the number of coatings increases, the porosity would decrease tending to reduce the transmission but the increased crystallinity and surface homogeneity will increase the transmittance. Under these contrasting effects, the transmittance may register a fall up to a certain film thickness and then may become more or less a constant. As a matter of fact, a near constancy of transmittance is found in  $\text{In}_2\text{O}_3$  films of the present study for the number of coatings between 7 and 10 (i.e. for the film thickness ranging between 225 and 292 nm). In every case, the transmittance falls very sharply at the lower wavelength region due to the onset of the fundamental absorption. The absorption edge has a minimum value of

359 nm at the 9th coating and the band gap value at this stage is 3.45 eV.

Thus, the XRD, electrical and optical studies support the influence of the number of coatings (i.e. film thickness) on the characteristics of the SGS coated  $\text{In}_2\text{O}_3$  films prepared in the present study and they further indicate that films with good optoelectronic characteristics are formed at 9 coatings.

### 3.3. Effect of heat treatment (process) temperature

Since the heat treatment of the SGS coated films is a very crucial step in obtaining crystalline transparent conducting oxide films, the influence of the heat treatment temperature on the characteristics of the prepared  $\text{In}_2\text{O}_3$  films has been investigated.

#### 3.3.1. Structural studies

The X-ray diffractograms of the SGS coated  $\text{In}_2\text{O}_3$  films prepared at different process temperatures of 400, 425, 450 and 475 °C are presented in Fig. 4b. These diffractograms indicate that all the films are polycrystalline and have bixbyte (bcc structure) with (222) orientation as the most dominant orientation which is in accordance with the standard data [42] for  $\text{In}_2\text{O}_3$ . The sharp and narrow peaks obtained for the  $\text{In}_2\text{O}_3$  films of the present study point to good crystallinity of the crystallites with a fairly large grain size. For the (222) orientation, the grain size works out to be 28.8 nm. This value is close to the value reported by Joseph Prince et al. [25] for their sprayed IO films.

The lattice constant comes out to be 10.11(1) Å which is in very good agreement with the value reported by Parent et al. [38] for  $\text{In}_2\text{O}_3$  crystals. The result of the present study that the (222) orientation is the dominant orientation for  $\text{In}_2\text{O}_3$  films at all process temperatures is similar to the results of Baba Ali et al. [43] and Joseph Prince et al. [25] for their  $\text{In}_2\text{O}_3$  films prepared at different process temperatures using reactive sputtering and spray pyrolysis preparation techniques, respectively. This also coincides with the contention of Mergel et al. [39] and Ghosh et al. [40] that the films prepared by processes which do not involve high-energy particle bombardment of growing films will have dominant (222) orientation only.

The predominant peak observed in all the patterns is due to the reflection from (222) plane of  $\text{In}_2\text{O}_3$  irrespective of the heat treatment temperature. These may be taken to indicate the presence of a close packed plane of oxygen in  $\text{In}_2\text{O}_3$  body-centered cubic structure as observed by Nagatoma et al. [44]. In addition, few other peaks with very weak intensities are also observed. This shows that these films have less number of crystallites having orientation other than (222) orientation. Further, all the allowed reflections of  $\text{In}_2\text{O}_3$  reported in the standard data are not observed. It is due to the fact that when the crystallites are sub-micron in size the reflections (peak intensity) from the corresponding lattice planes will be either of very low value or too weak to be observed by powder XRD analysis.

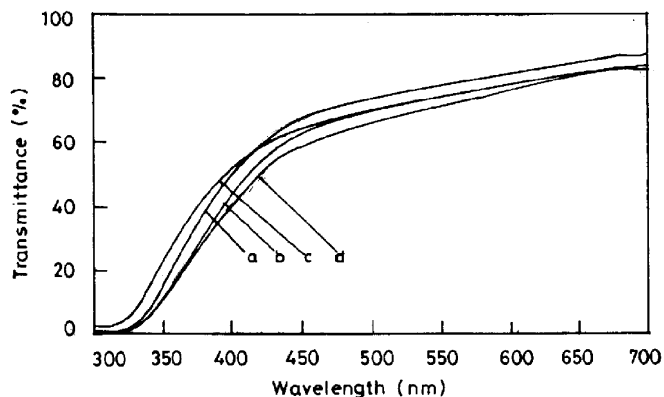


Fig. 6. Transmittance spectra of IO films with different number of coatings: (a) 7; (b) 8; (c) 9; and (d) 10 coatings.

These observations elucidate the presence of sub-micron size crystallites in the SGS coated  $\text{In}_2\text{O}_3$  films. It can also be explicitly observed that the XRD patterns of  $\text{In}_2\text{O}_3$  films do not show peaks pertaining to intermediates such as  $\text{In}_x\text{O}_y$  or other suboxides of indium like  $\text{In}_2\text{O}$ . This once again confirms the monophasic nature of the indium oxide films prepared in the present work. As the heat treatment temperature increases, the intensities of (222), (400), (211), [411] and (622) peaks increase up to 425 °C. This indicates that there could be marked improvement in the crystallinity and size of the crystallites. When the heat treatment temperature is increased beyond 425 °C, the intensity of the (222) peak falls while the intensity of (400) peak increases at a slow rate. This may point to some sort of local disorder/atomic rearrangement in the crystallites beyond 425 °C. Such a trend that the XRD intensity increases up to certain process temperature and then falls is explicitly seen in Fig. 4b. It may be attributed to the variation in the amount of oxygen intake and energy of ad atoms [45]. The mobility of ad atoms and clusters on the surface of substrates is proportional to their energy, which increases with increasing substrate temperature. This will lead to the growth of  $\text{In}_2\text{O}_3$  crystallites with simple crystal planes like (100). Further, the substrate temperature would modify the reactivity of indium precursor with  $\text{O}_2$  thereby controlling the film growth process itself.

### 3.3.2. Electrical studies

The Hall effect measurements indicate that all the spin coated  $\text{In}_2\text{O}_3$  films prepared at different temperatures are n-type semiconductors. The carrier concentration ( $n$ ), the mobility ( $\mu$ ) and resistivity ( $\rho$ ) of the films as a function of heat treatment temperature are shown in Fig. 7. The figure indicates that the carrier density and mobility increase as the process temperature increases up to 425 °C and then falls; the resistivity falls up to 425 °C and then rises. Such trends have been reported by Joseph Prince et al. [25] and Vasu and Subramanyam [46] for their sprayed  $\text{In}_2\text{O}_3$  films. The reasonably high carrier density of the spin coated  $\text{In}_2\text{O}_3$  films ( $n = 1.88 \times 10^{19} \text{ cm}^{-3}$ ) at a relatively high temperature of 475 °C may be attributable to the presence

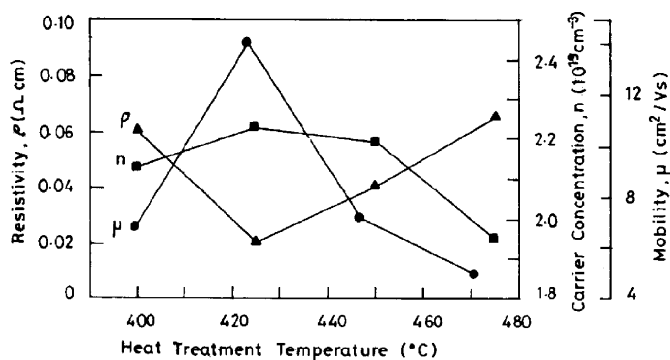


Fig. 7. Variation of carrier concentration ( $n$ ), mobility ( $\mu$ ) and resistivity ( $\rho$ ) of IO films (9 coatings) with heat treatment temperatures.

of some oxygen vacancies and/or excess indium atoms acting as charge donor centers [47]. As pointed out by Noguchi and Sakata [47] the high value for the concentration of the carrier electrons at these temperatures may be due to the atoms excited thermally from the defects near the bottom of the conduction band. Further, the fairly high value of  $2.22 \times 10^{19} \text{ cm}^{-3}$  for the carrier concentration for the optimized spin coated  $\text{In}_2\text{O}_3$  films of the present study indicates that the films are highly degenerate as the onset of degeneracy starts at a carrier density of  $1.48 \times 10^{18} \text{ cm}^{-3}$  for the IO single crystal [39].

The Fermi energy  $E_F$  of the film can be calculated using the relation

$$E_F = \left( \frac{h^2}{8m^*} \right) \left( \frac{3N}{\pi} \right)^{2/3}, \quad (3)$$

taking  $m^*$  as  $= 0.3m_0$ ,  $E_F = 0.1 \text{ eV}$  and  $KT = 0.02 \text{ eV}$ ,  $E_F \gg KT$ . This result also indicates that the  $\text{In}_2\text{O}_3$  films of the present study are degenerate semiconductors. This is consistent with the conclusion arrived at by Noguchi and Sakata [47] for their reactively evaporated  $\text{In}_2\text{O}_3$  films and Vasu and Subramanyam [46] and Joseph Prince et al. [25] for their sprayed  $\text{In}_2\text{O}_3$  films. The Hall mobility ( $\mu$ ) is fairly low when compared to the values reported by Noguchi and Sakata [47], Chopra et al. [4] and Joseph Prince et al. [25] for their indium oxide films developed using other preparation methods. The grain boundary scattering may influence the mobility. The mean free path of a free carrier is given by

$$l = (h/2e)(3N/\pi)^{1/3}\mu. \quad (4)$$

The mean free path for the spin coated  $\text{In}_2\text{O}_3$  films is found to be 0.802 nm ( $n = 2.22 \times 10^{19} \text{ cm}^{-3}$  and  $\mu = 14.0 \text{ cm}^2/\text{Vs}$  (at a process temperature = 425 °C), which is considerably shorter than the grain size of 28.8 nm. This means that the grain boundary scattering is not the only mechanism reducing the mobility of the free carriers in these films. The possibility is that there could be the presence of other scattering process such as impurity scattering and lattice scattering in addition to grain boundary scattering as pointed out by Noguchi and Sakata [47], Chopra et al. [4], Bel Hadj Tahar et al. [48] and Baba Ali et al. [43]. At 425 °C the carrier density and mobility are maximum ( $n = 2.22 \times 10^{19} \text{ cm}^{-3}$  and  $\mu = 14.0 \text{ cm}^2/\text{Vs}$ ) and resistivity minimum (0.020  $\Omega \cdot \text{cm}$ ). The XRD studies given earlier indicate that there is improvement in crystallinity and size of the crystallites from 400 to 425 °C which will tend to improve the electrical characteristics. This effect may be more than the impeding effect due to decrease in oxygen vacancies and hence the carrier concentration, mobility and conductivity would increase up to 425 °C. Beyond 425 °C there is disorder/atomic rearrangement in the crystallites as indicated by the XRD studies which becomes an additional impeding factor. The possible dominance of these impeding factors over the aiding factor would result in the overall reduction in the electrical characteristics of the film beyond

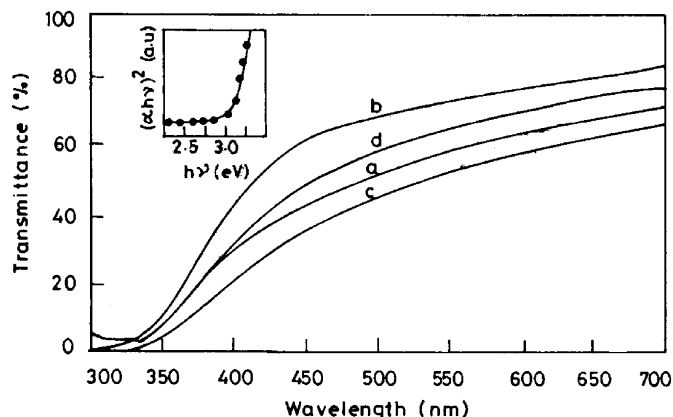


Fig. 8. Transmittance spectra of IO films (9 coatings) with different heat treatment temperatures: (a) 400 (b) 425, (c) 450, and (d) 475 °C. Insert shows  $(\alpha h\nu)^2$  vs.  $h\nu$ .

425 °C. Thus, the electrical studies indicate that the best  $\text{In}_2\text{O}_3$  thin films can be obtained at 425 °C using the SGS coating technique.

### 3.3.3. Optical studies

The transmittance spectra of the  $\text{In}_2\text{O}_3$  films prepared at 400, 425, 450 and 475 °C are shown in Fig. 8. The figure shows that the transmittance in the visible region is maximum at 425 °C and then it falls. When the process temperature increases from 400 to 425 °C films with steeper absorption in the UV region are obtained. Such results have been reported by Vasu and Subramanyam [46] and Joseph Prince et al. [25] for their sprayed films. The increase in visible transmittance of the film with temperature may be attributable to the improvement in the crystallinity of the crystallites and improvement in the

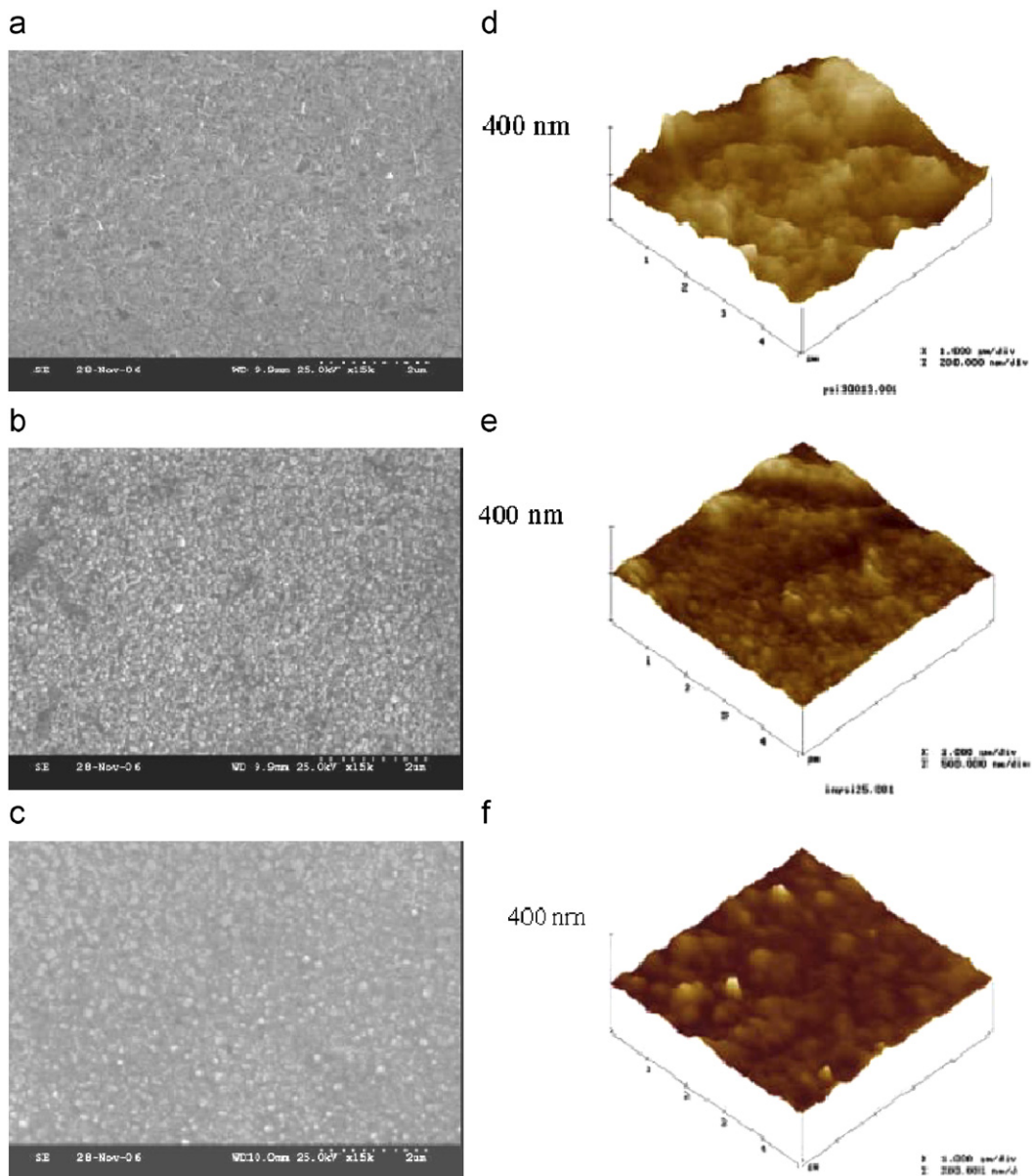


Fig. 9. SEM (a–c) pictures and AFM (d–f) images of IO films (9 coatings) heat treated at 400, 425 and 450 °C, respectively.

structural and surface homogeneity of the films [44]. The reduction in the transmittance after 425 °C may be due to some sort of disorder or impairment in the crystallinity of the films as evidenced from the XRD studies. The same conclusion has been arrived at by Joseph Prince et al. [25] for their sprayed In<sub>2</sub>O<sub>3</sub> films. At 425 °C the transmittance is maximum (80%), the absorption edge shows a minimum (359 nm) and the band gap a maximum of 3.45 eV which is close to the value reported for bulk In<sub>2</sub>O<sub>3</sub> by Chopra et al. [4].

The linearity of  $(\alpha hv)^2$  vs. energy ( $hv$ ) plot for the process temperature of 425 °C (insert in Fig. 8) and the value of  $\alpha$  of the order of  $10^4$  confirm that the absorption near the fundamental edge is due to direct allowed transition.

### 3.4. Surface morphological studies

The spin coated In<sub>2</sub>O<sub>3</sub> films heated at 425 °C are highly uniform and homogenous with regard to the surface topography and thickness over an area of 1 cm × 1 cm as observed by the SurfTest SJ-301 stylus-type surface roughness and thickness measuring instruments.

SEM and AFM were used for the study of surface morphological changes observed on the surface of In<sub>2</sub>O<sub>3</sub> films prepared at 400, 425 and 450 °C. The SEM pictures show that the films are uniform, well adherent and completely devoid of pin holes and cracks. Film heated at 400 °C (Fig. 9a) has smooth surface and no grains were perceptible. At 425 °C (Fig. 9b) of heating the surface starts to modify and smaller granular particles found uniformly distributed all over the surface with a size of about 0.12 μm. When the heating temperature is increased to 450 °C (Fig. 9c), the surface becomes inhomogenous probably from the clustering of the small grains with the size varying between 0.18 and 0.22 μm. Fig. 9d shows the surface topographical image of the In<sub>2</sub>O<sub>3</sub> films heated at 400 °C, which is highly non-uniform due to the presence of large conglomerate patches with an average root mean square (RMS) roughness of 58 nm. Films have homogenous uniform surface at 425 °C (Fig. 9e) that are composed of spherical granules of 250 nm dimension with very little porosity and there are no agglomerations in the films. An even surface roughness is observed with an average RMS value of 27 nm. It is inferred from the AFM micrograph (Fig. 9f) of IO film prepared at 450 °C that the surface becomes inhomogenous with increased heating temperature and the grain size seems to increase (400–600 nm) due to the coalescing of the smaller grains observed at 425 °C. This leads to an increasingly rough surface with very porous and larger granular morphology whose RMS roughness value is 42 nm.

## 4. Conclusion

This first ever results on the SGS coated In<sub>2</sub>O<sub>3</sub> films indicate that 425 °C is the optimum temperature with optimized number of coatings of 9 for producing quality

films. The values of  $n = 2.12 \times 10^{19} \text{ cm}^{-3}$ ,  $\mu = 14.0 \text{ cm}^2/\text{Vs}$ ,  $\rho = 0.02 \Omega \text{ cm}$ , transmittance 80% and  $E_g = 3.45 \text{ eV}$  obtained for the SGS coated In<sub>2</sub>O<sub>3</sub> films are in the range of values reported by other investigators [5,25,47] for their In<sub>2</sub>O<sub>3</sub> films prepared by other preparation techniques. Only the resistivity appears to be a little lower than the values obtained using other preparation techniques; nevertheless, it is in the range of values useful for the device preparation. To reduce the resistivity further and also to increase the transmission behavior of the SGS coated In<sub>2</sub>O<sub>3</sub> films, studies on the effect of annealing in vacuum and in argon + hydrogen ambient are in progress.

## References

- [1] O. Warschkow, D.E. Ellis, G.B. Gonzalez, T.O. Manson, J. Am. Ceram. Soc. 86 (2003) 1700.
- [2] S. Marsillac, P.D. Paulson, M.W. Haimbodi, R.W. Birkmire, W.N. Shafarman, Appl. Phys. Lett. 81 (2002) 1350.
- [3] N. Biyikli, I. Kimukin, T. Kartaloglu, O. Aytur, E. Ozbay, Appl. Phys. Lett. 82 (2003) 2344.
- [4] K.L. Chopra, S. Major, D.K. Pandya, Thin Solid Films 102 (1983) 1.
- [5] C.G. Granquist, Sol. Energy Mater. Sol. Cells 60 (2000) 2301.
- [6] A.N.H. Ajili, S.C. Bayliss, Thin Solid Films 305 (1997) 116–123.
- [7] I. Hamberg, C.G. Granqvist, J. Appl. Phys. 60 (1986) R123.
- [8] G. Eftekhari, Semicond. Sci. Technol. 10 (1995) 1159.
- [9] A. Golan, Y. Shapira, M. Eizenberg, J. Appl. Phys. 72 (1992) 925.
- [10] V. Korobov, Y. Shapira, B. Ber, K. Faleev, D. Zushinskiy, J. Appl. Phys. 75 (1994) 2264.
- [11] S.A. Bashar, A.A. Rezazadeh, IEEE Trans. Microw. Theor. Tech. 43 (1995) 2299.
- [12] G. Kiriakidis, H. Ouacha, N. Katsarakis, Rev. Adv. Mater. Sci. 4 (2003) 32.
- [13] R. Winter, K. Schamagl, A. Fuchs, T. Doll, I. Eisele, Sens. Actuators B 66 (2000) 85.
- [14] G. Kiriakidis, N. Katsarakis, M. Bende, E. Gagaoudakis, V. Cimalla, Mater. Phys. Chem. 1 (2000) 83.
- [15] H. Fritzsche, B. Pashmakov, B. Clafin, Sol. Energy Mater. Sol. Cells 32 (1994) 383.
- [16] P. Tuner, R.P. Howson, C.A. Bishop, Thin Solid Films 83 (1981) 253.
- [17] S. Suh, D.M. Hoffmann, J. Am. Chem. Soc. 122 (2000) 9396.
- [18] M. Mizuhashi, Thin Solid Films 70 (1980) 91.
- [19] C.A. Pan, T.P. Ma, Appl. Phys. Lett. 37 (1980) 163.
- [20] E.J. Tarsa, J.H. English, J.S. Speck, Appl. Phys. Lett. 62 (1993) 2332.
- [21] C. Grivas, D.S. Gill, S. Mailis, L. Boutsikaris, N.A. Vainos, Appl. Phys. A 66 (1998) 21.
- [22] J.-S. Cho, K.H. Yoon, S.-K. Koh, J. Appl. Phys. 89 (2001) 3223.
- [23] A.N.H. Al-Ajili, S.C. Bayliss, Thin Solid Films 305 (1997) 116.
- [24] D.V. Morgan, Z.H. Aliyu, R.W. Bunce, A. Sakhi, Thin Solid films 312 (1998) 268.
- [25] J. Joseph Prince, S. Ramamurthy, B. Subramanian, C. Sanjeevaraja, M. Jayachandran, J. Cryst. Growth 240 (2002) 142.
- [26] J.C. Manificier, Thin Solid Films 90 (1982) 297.
- [27] D. Yu, D. Wang, T. Qian, J. Solid State Chem 177 (2004) 1230.
- [28] M. Girtan, G.I. Rusu, Mater. Sci. Eng. 676 (2000) 156.
- [29] H. Imami, A. Tominaga, H. Hirashima, S. Toki, N. Asakuma, J. Appl. Phys. 85 (1999) 203.
- [30] Y.J. Lin, C.J. Wu, Surf. Coat. Technol. 88 (1996) 239.
- [31] C. Cobianu, C. Savaniu, O. Buiu, D. Dascalu, M. Zaharescu, C. Parlog, A. Berg, B. Peez, Sensors Actuators B 43 (1997) 114.
- [32] E. Savarimuthu, N. Sankarasubramanian, B. Subramanian, M. Jayachandran, C. Sanjeeviraja, S. Ramamurthy, Surf. Eng. 224 (2006) 268.
- [33] W.J. Daughton, F.L. Givens, J. Electrochem. Soc. Solid State Sci. Technol. 129 (1985) 173.

- [34] S. Hirasawa, Y. Saito, H. Nezu, N. Ohashi, H. Maruyama, *IEEE Trans. Semiconduct. Manufact.* 4 (1997) 438.
- [35] L.M. Peurrung, D.B. Graves, *IEEE Trans. Semiconduct. Manufact.* 6 (1) (1993) 72.
- [36] S.C. Lee, J.H. Lee, T.S. Oh, Y.-H. Kim, *Sol. Energy. Mater. Sol. Cells* 75 (2003) 481.
- [37] N. Sankarasubramanian, E. Savarimuthu, C. Sanjeeviraja, S. Ramamurthy, *Trans. SAEST* 40 (2005) 62.
- [38] Ph. Parent, H. Dexpert, G. Tourillon, J.M. Grimal, *J. Electrochem. Soc.* 139 (1992) 276.
- [39] D. Mergel, M. Schenkel, M. Ghebre, M. Sulkowski, *Thin Solid Films* 392 (2001) 91.
- [40] S. Ghosh, H. Kim, K. Hong, C. Lee, *J. Mater. Sci. and Eng. B* 95 (2002) 171.
- [41] S.S. Kim, S.-Y. Choi, C.-G. Park, H.-W. Jin, *Thin Solid Films* 347 (1999) 155.
- [42] Powder Diffraction File, PCPDFWIN Version 1. 30 JCPDS-ICDD, Pennsylvania, 1997, Card 06-0416.
- [43] E. Baba Ali, G. Sorensen, J. Ouerfelli, J.C. Bernede, H. El. Maliki, *Appl. Surf. Sci.* 152 (1999) 1.
- [44] T. Nagatoma, Y. Maruta, O. Omoto, *Thin Solid Films* 192 (1990) 17.
- [45] L.J. Meng, M.P. Dos Santos, *Thin Solid Films* 322 (1998) 56.
- [46] V. Vasu, A. Subramanyam, *Thin Solid Films* 193/194 (1990) 696.
- [47] S. Noguchi, Sakata, *J. Phys. D* 13 (1980) 1129.
- [48] R. Bel HadjTahar, T. Ban, Y. Ohya, Y. Takahashi, *J. Appl. Phys.* 83 (1998) 2631.